IOP Publishing Measurement Science and Technology
Meas. Sci. Technol. **28** (2017) 107001 (6pp) https://doi.org/10.1088/1361-6501/aa5f9c

Technical Note

Two simple modifications to improve the magnetic field profile in radial magnetic systems

Shisong Li[1,2] **and Stephan Schlamminger**[1]

[1] National Institute of Standards and Technology, Gaithersburg, MD 20899, United States of America
[2] International Bureau of Weights and Measures (BIPM), Pavillon de Breteuil, F-92312 Sèvres Cedex, France

E-mail: leeshisong@sina.com and stephan.schlamminger@nist.gov

Received 3 November 2016, revised 6 February 2017
Accepted for publication 9 February 2017
Published 12 September 2017

Abstract

All present watt balances employ permanent magnet systems using a yoke with high permeability as flux return. Very often these systems are built with vertical and azimuthal symmetries. In its simplest form, the air gap is defined as the radial distance between an inner and outer yoke with the same height. This design leads to sloped field lines away from the plane of vertical symmetry. In order to suppress this vertical magnetic field, we propose two modified magnet constructions: (1) adding a permanent magnet in the outer yoke, and (2) decreasing the height of the outer yoke. Finite element method simulations show that, with reasonable optimization, either proposal can lower the vertical magnetic field by about one order of magnitude.

Keywords: watt balance, alignment, magnetic field

(Some figures may appear in colour only in the online journal)

1. Watt balance magnet

The watt balance [1] is an instrument for realizing a unit of mass, the kilogram [2], in the revised International System of Units (SI) [3]. A summary of the worldwide development of watt balance experiments can be found in [4–6]. Traditionally, two measurement modes are used in the operation of a watt balance: in the weighing mode, the weight of a test mass, mg, is balanced by an electromagnetic force $BlI = mg$, where m, g, B, l and I denote the mass of the test mass, the local gravitational acceleration, the magnetic flux density at the coil position, the coil wire length and the current through the coil, respectively. In the velocity mode, the coil is moved with a velocity v through the same magnetic field, inducing an electromotive force (EMF) U, and the Bl can be obtained as $Bl = U/v$. An elimination of the factor Bl in both modes yields a virtual power balance equation, $mgv = UI$, by which the mass m is linked to the Planck constant h via measurements of the voltage, the resistance, the time and the length, see e.g. [7] for details.

An assumption of the watt balance experiment is that the geometric factor Bl (integral of the magnetic flux density along the coil wire path) is the same in weighing as it is in velocity mode. Since the exact coil position is hard to control in velocity mode, it is important to design a magnet whose Bl is insensitive to the exact location (x, y, and z) and orientation (θ_x, θ_y, and θ_z) of the coil. For example, if the horizontal magnetic flux density B_r is proportional to $1/r$ ($r = \sqrt{x^2 + y^2}$ is the radial distance), the Bl is independent of x and y. Gauss' law links the vertical component of the magnetic flux density to the horizontal component and as a consequence $B_r \propto 1/r$ can be achieved with $B_z = 0$ in the entire field volume. With these two requirements, the geometric factor is independent to the coil horizontal movement, wire deformation [8] and yoke

misalignment [9]. If B_z does not vanish, Bl will depend on the remaining degrees of freedom of the coil $(x, y, \theta_x, \theta_y)$, and in this case the mechanical system must be very well designed to avoid coil motion along these degrees of freedom during the velocity mode. Conversely, a magnet with a geometric factor that is independent of these coordinates allows the use of a simpler mechanical system, effectively relaxing the requirements for aligning the coil to the magnetic field.

Recently, permanent magnets with high permeability yokes have been the preferred magnet system in watt balances at various laboratories [10–17]. A popular design is the BIPM type magnet, pioneered by the group working at the Bureau International des Poids et Mesures (BIPM). This design employs two opposing permanent magnets, shown in figure 1(a). A detailed construction of such magnets can be found in [14]. Generally, the magnetic flux of the permanent magnets is guided by yokes horizontally through an air gap, where the coil is located. The air gap has the shape of a cylindrical shell. Its inner and outer boundaries are given by the inner and outer yokes. Typically, the heights of the inner yoke and outer yoke are the same.

2. Problem

It has been shown in [18] that a magnet design depicted in figure 1(a) will create a noticeable vertical component of the field B_z, which has to be considered for the coil alignment. Figure 2 shows the contribution of $rB_r(r, z)/r_c$, where r_c is the radius of the center of the air gap and $B_z(r, z)$ based on simulations using the finite element method (FEM) of a BIPM type magnet used in the fourth generation watt balance experiment at the National Institute of Standards and Technology (NIST-4) [14]. The vertical magnetic component B_z in the air gap center is about 3 mT at $|z| = 50$ mm, i.e. 0.6% of the horizontal magnetic component. $B_z(r)$ reaches a maximum value near the center of the air gap $r = r_c$, see figure 2(b), which is different from the field contribution of a classic two parallel plate, where $B_z \approx 0$ in the center of the gap center. This difference is caused by the asymmetry of inner and outer yoke–air boundaries. Figure 1(a) shows the inner/outer yoke-air boundary in pink/green respectively, while the magnet–air surface is highlighted in red. At least two asymmetries are apparent: first, the parallel boundary (red air-magnet surface) exists only on the surface of inner side. Second, the outer yoke–air particular boundary is much longer than that of the inner yoke side. Together these asymmetries will create a sloped magnetic flux towards the ends of the air gap and as a result produce a vertical field component $B_z(r,z)$ as shown in figure 2(b).

3. Solutions

We propose two different methods to suppress the unwanted vertical flux density B_z. The first approach is to add a second pair of permanent ring magnets to restore the symmetry of the air-yoke and air-magnet boundaries. The second is to change the heights of the inner and outer yokes.

3.1. Approach 1: adding permanent magnets

Figure 1(b) shows the construction of a magnet system that has permanent magnets added to the outer yoke. This will divide the outer yoke into three separate parts, the upper, middle and lower segments. Since the upper and lower segments perform as the common yoke of both inner and outer yokes, it is possible to adjust the inner yoke and the middle segment of the outer yoke to make the air gap magnetically symmetrical. A simple estimation of the step widths a and b is based on an assumption that the ratio of the flux through both steps to the flux through the corresponding magnets is the same on both sides of the air gap. This requires

$$\frac{a}{b} \approx \frac{l_a}{l_b}, \tag{1}$$

where l_a and l_b are the widths of the inner and outer permanent magnets, shown in figure 1(b). In order to verify equation (1), a FEM simulation has been performed. Two additional permanent magnets are set at the same height of the original pair. $a = 30$ mm, $b = 14$ mm, $l_a = 120$ mm and $l_b = 56$ mm. The simulation result is shown in figure 3. The vertical component of the field in the entire air gap region has been greatly reduced. The improvement can be quantified with a figure of merit, the average absolute value (aav) of the vertical flux density B_{aav} defined as

$$B_{\text{aav}} := \frac{\int_{z_1}^{z_2}\int_{r_i}^{r_o} |B_z(r,z)|\,\mathrm{d}r\mathrm{d}z}{\int_{z_1}^{z_2}\int_{r_i}^{r_o} \mathrm{d}r\mathrm{d}z}, \tag{2}$$

where the integrals are evaluated over the nominal extent of the air gap, accessible by the coil, given by $r \in (r_i, r_o)$ and $z \in (z_1, z_2)$. The B_{aav} of the two designs shown on the left of figure 1 are calculated to be 0.44 mT and 0.066 mT in the region $z \in (-50$ mm, 50 mm), $r \in (200$ mm, 230 mm). By using additional permanent magnets, the average absolute value of the vertical flux density is reduced to about 15% of the original value while the peak value of B_z is reduced by more than an order of magnitude.

Adding a permanent magnet into the outer yoke also has a significant disadvantage: the shielding of the yoke is compromised. In the original design, the coil is completely enclosed in iron. Magnetic fields from the outside generated by alternating currents cannot reach the coil. This is no longer true after the set of outer ring magnets have been added.

3.2. Approach 2: lowering outer yoke height

The second method to suppress the vertical field component is based on a compensation idea. By creating an additional magnetic flux pointing to the center of the outer yoke, the original flux pointing to the end of the outer yoke can be compensated, yielding a flat B_z profile. One approach is to shorten the height of the outer yoke, i.e. by designing $H_i > H_o$ where H_i and H_o denote the height of the inner and outer yokes, shown in figure 1(c). This idea was implemented in the original BIPM design, see [19]. Another FEM is used to test this idea. For this FEM, all other parameters

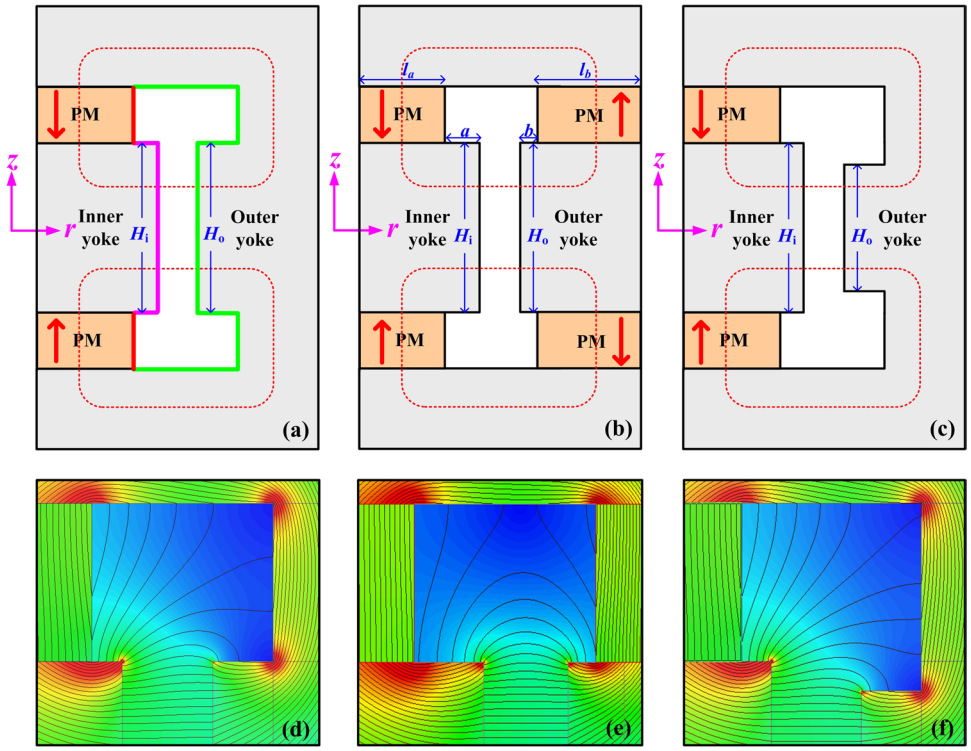

Figure 1. The upper subplot shows three different designs for watt balance magnets. In (a)–(c), only the right half cross section is shown. In these plots, PM denotes the magnetic material and the red arrow denotes the magnetization direction. The red dotted line shows the main flux flow path. (a) is a conventional construction with two permanent magnets and equal heights of the inner and outer yoke, i.e. $H_i = H_o$. (b) is the modified construction with four permanent magnets and identical heights for both yokes. (c) is a construction with two permanent magnets and a lower height of the outer yoke, i.e. $H_i > H_o$. The lower subplots show the magnetic flux lines at the upper end of the air gap. (d)–(f) correspond to the designs (a)–(c).

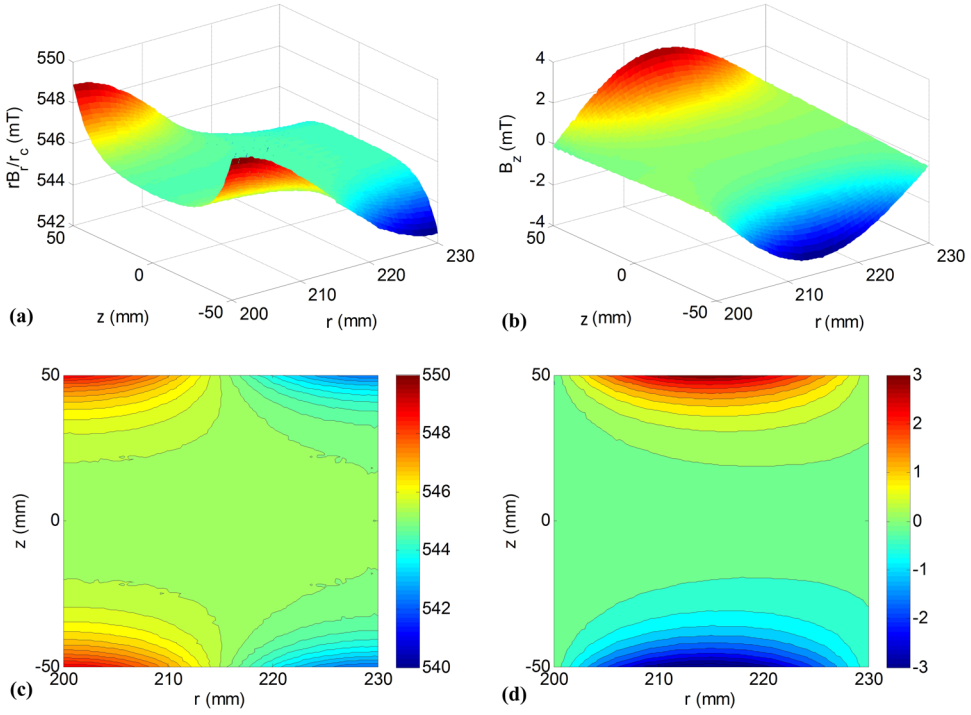

Figure 2. Calculation results of magnetic flux density distribution of figure 1(a). (a) is the 3D magnetic flux density distribution of $rB_r(r, z)/r_c$ (r_c is the radius of the air gap center) while (b) shows the 3D magnetic flux density distribution of $B_z(r, z)$. The focused region is $z \in (-50\,\text{mm}, 50\,\text{mm})$, $r \in (200\,\text{mm}, 230\,\text{mm})$. (c) and (d) are 2D plots of (a) and (b) in mT. The height and width of the air gap is $H = 170\,\text{mm}$ and $\delta_0 = 30\,\text{mm}$ in NIST-4 magnet.

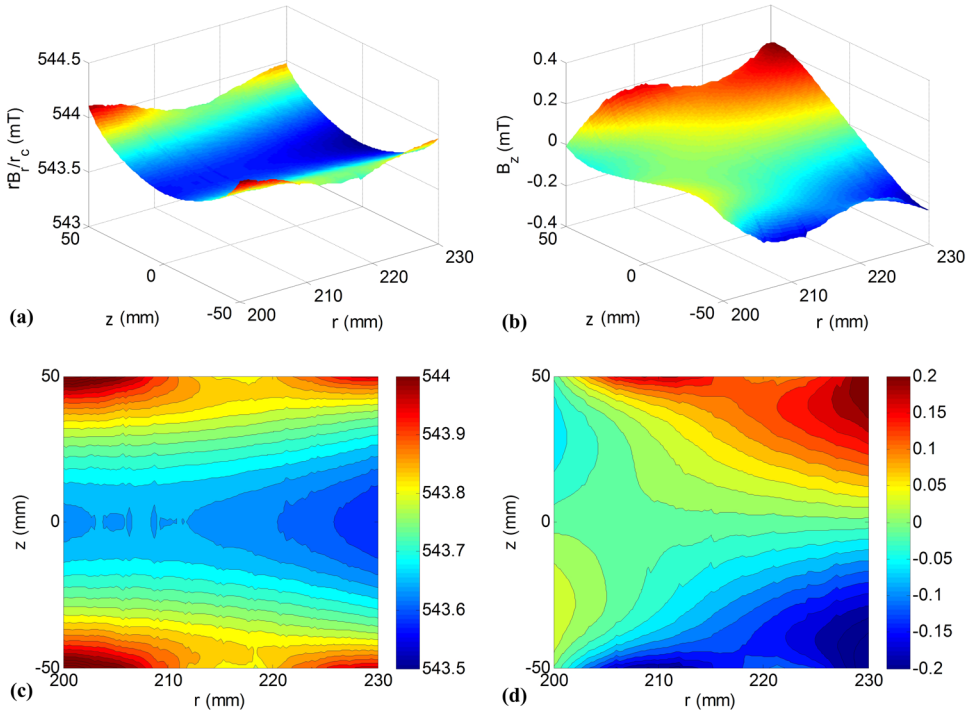

Figure 3. Calculation results of the magnetic flux density distribution of a construction shown in figure 1(b). (a) is the 3D magnetic flux density distribution of $rB_r(r, z)/r_c$ while (b) shows the 3D magnetic flux density distribution of $B_z(r, z)$. (c) and (d) are 2D plots of (a) and (b) in mT with $a = 30$ mm, $b = 14$ mm, $l_a = 120$ mm and $l_b = 56$ mm.

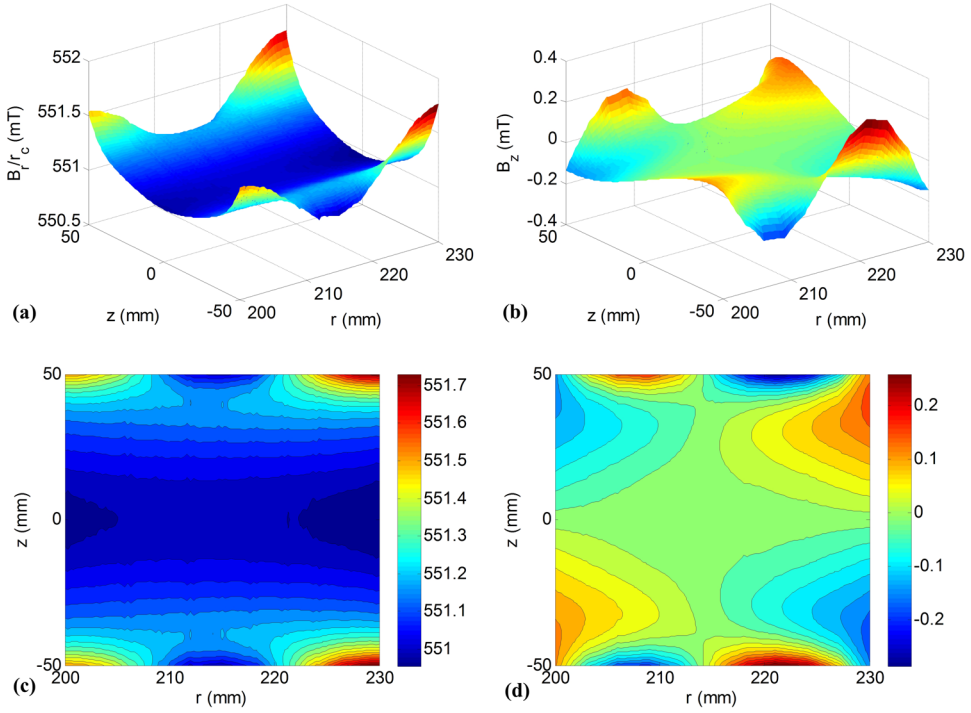

Figure 4. Calculation results of the magnetic flux density distribution of a construction shown in figure 1(c). (a) is the 3D magnetic flux density distribution of $rB_r(r, z)/r_c$ while (b) shows the 3D magnetic flux density distribution of $B_z(r, z)$. (c) and (d) are 2D plots of (a) and (b) in mT. $H_i = 170$ mm, $H_o = 151$ mm.

are kept the same as in figure 1(a) except H_o which is set as a variable. From the simulation, an optimal height of $H_o = 151$ mm has been found yielding a $B_{\text{aav}} = 0.046$ mT, about an order of magnitude smaller than the original design with $H_o = 170$ mm. The results of the FEM are shown in figure 4.

A good way to obtain the ideal height of H_o would be to find an analytic solution in the air gap region. A calculation using an equivalent electrostatic field, shown in figure 5(a), has been attempted. The boundary condition has been met, however it is still difficult to give an analytic formula for H_o as a function of the air gap dimensions.

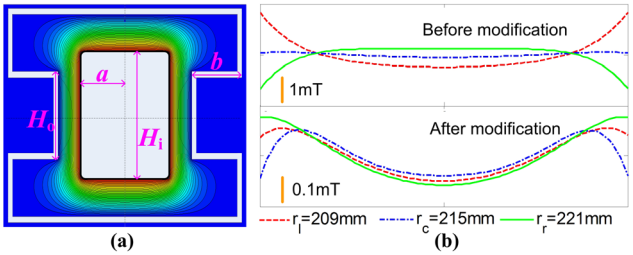

Figure 5. (a) Presents an electrostatic field problem with similar solutions of the magnetic contribution in the air gap of watt balance magnets. The image axis is $r = r_m$ where r_m is the outer radius of the permanent magnet. (b) Shows a comparison of three different $B_r(r, z) - B_a$ profiles, where B_a is the mean value of $B_r(r, z)$, with $r = r_l$, r_c and r_r before and after modifications.

Short of an analytic equation, the best outer yoke height can be found by iteration. The magnet system of a watt balance can be assembled and disassembled without major change. The achieved flatness of the field magnetic field can be measured and adjusted. One way to measure the field flatness is by using a field sensing coil made up by three stacked pairs of gradient coils with mean radii r_l, r_c and r_r [14] to measure the gradient of $B_r(r_l, z)$, $B_r(r_c, z)$ and $B_r(r_r, z)$ profiles. Figure 5 shows the simulated results of an example with $r_l = 209\,\text{mm}$, $r_c = 215\,\text{mm}$ and $r_r = 221\,\text{mm}$, before and after modification of the outer yoke height H_o. It can be seen with a well optimized H_o (lower graph) that the gradients of three profiles $B_r(r_l, z)$, $B_r(r_c, z)$ and $B_r(r_r, z)$ are comparable, while in a bad case (upper graph), the three magnet flux densities differ by about 1 mT. Therefore, the gradient consistency of the three $B_r(z)$ profiles can be used as a figure of merit to find the best H_o value.

4. Discussion

Both solutions presented here require small deviation from the BIPM type magnet design. The first solution requires a substantial change, i.e. the addition of two ring magnets in the outer yoke. This solution will add to the manufacturing cost and compromise the shielding property of the magnet system. The second solution, which only requires a change of the height of the outer yoke, was already incorporated in the original BIPM magnet design.

4.1. Magnetic field strength

In these magnet systems, the magnetic flux through the air gap is determined by the magnetomotive force and the reluctance of three different parts, the air gap, the permanent magnet and the yoke. With an up-down symmetrical construction, only half of the magnet needs to be considered. The magnetic equation of either half can be written as

$$\phi\left(\frac{\delta_0}{\mu_0 S_0} + \frac{\delta_m}{\mu_0 S_m} + \frac{\delta_y}{\mu S_y}\right) = H_m \delta_m, \tag{3}$$

where ϕ is the magnetic flux through the upper/lower air gap. δ_0, δ_m, δ_y denote the air gap width, the permanent height and the yoke average length along flux lines, and S_0, S_m, S_y are the sectional area of the upper/lower air gap, the permanent and the yoke. The permeability of the vacuum is given by μ_0 and μ is the permeability of the yoke, $\mu = \mu_r \mu_0$. H_m is the magnetic field strength of the permanent magnet in the vertical direction. Since $\mu \gg \mu_0$, the magnetic flux or B_r is mainly determined by the reluctance of the air gap and the permanent magnet. Modifying the height of the outer yoke reduces S_0 and S_y slightly, resulting in a very small increase in the magnetic flux in the gap. To calculate the effect of adding a magnet ring on the outer yoke in one half of the magnet, we make the following simplifications, $S_0 \approx S_m$ and $\delta_0 \approx \delta_m$. This approximation is justified, since the design of most magnet systems is such that the area and thickness of the permanent magnetic material and the gap are similar. Hence equation (3) simplifies to

$$\phi\left(2\frac{\delta_m}{\mu_0 S_m}\right) \approx H_m \delta_m. \tag{4}$$

With this simplification, the magnetic flux seems to be independent of the thickness of the magnet. However, by introducing a permanent magnet ring in the outer yoke, the magnet thickness will be doubled, while the reluctance increases by 50%, i.e.

$$\phi\left(3\frac{\delta_m}{\mu_0 S_m}\right) \approx 2H_m \delta_m. \tag{5}$$

Hence the magnetic flux through the air gap will increase by approximately 17%, i.e. the difference between 2/3 and 1/2.

4.2. Adjusting the radial magnetic flux profile

Very often the magnetic field profile, $B_r(z)$, of the manufactured magnet differs from the desired field profile. Several shimming methods can be used to modify the field profile. For example, the magnet can be disassembled and the yoke can be precision ground to change the field profile. This is usually done by increasing the gap size in regions where the field is larger. Another method, described in [14], takes advantage of the hysteresis properties of the yoke. The idea is to shift the yoke *BH* working point by partially changing the main flux path through the yoke based on the hysteresis feature of the yoke material. A *BH* point shift can increase the reluctance of the yoke, i.e. $\delta_y/(\mu S_y)$, so that the magnetic flux density can be reduced in the original stronger part. Since the percentage of the yoke reluctance and the total magnetic reluctance remains more or less of the same order (see the analysis in section 4.1), these methods can be also used with both modifications proposed here.

4.3. Magnetic field change in the weighing mode

In the weighing mode of a watt balance, the flux generated by the current-carrying coil will be added to the flux produces by the permanent magnet system. This flux yields an additional force in the measurement, which is known as the reluctance force. Note that the majority of the additional coil flux will

go directly through the air gap (twice), the inner yoke and the outer yoke. The magnetic equations for the additional flux can be written as

$$\phi_c\left(\frac{\delta_0}{2\mu_0\pi r_c(H/2+z)}+\frac{\delta_0}{2\mu_0\pi r_c(H/2-z)}\right)=NI, \quad (6)$$

where ϕ_c is the additional flux generated by the coil, r_c the center radius of the air gap, H the full yoke height, z the coil vertical position, and N the coil number of turns. Based on equation (6), the reluctance force can be solved as

$$f_r=\frac{I^2}{2}\frac{\partial(N\phi_c/I)}{\partial z}=-\frac{2\pi\mu_0 I^2N^2r_cz}{\delta_0 H}. \quad (7)$$

It can be seen from equation (7) that the reluctance force is determined by the air gap dimension and the ampere turns squared. The modification proposed in figure 1(b) leaves the air gap unchanged. Hence, the reluctance force will be identical to the original design. For the other solution, shown in figure 1(c), the outer yoke is shortened. This will increase the reluctance force by a few percent.

5. Summary

Yoke-based permanent magnet systems are widely used in watt balances. In a design where the inner and outer yokes have the same height, a large vertical component of the field can arise. This vertical component is caused by an asymmetry of the magnet–air boundary between the inner and outer yoke. A reduction of the vertical component of the magnetic field is desired for several reasons: this reduction decreases the alignment error, increases the parameter space for the coil radius, and extends the region of the flat $B_r(z)$ profile.

Two solutions to minimize the vertical flux density have been proposed: (1) adding a permanent magnet in the outer yoke, and (2) decreasing the height of the outer yoke. FEM simulations show the effectiveness of both solutions. The vertical component can be reduced by almost one order of magnitude by either solution.

The ideas to flatten the magnetic field were analyzed using the BIPM magnet design. This analysis can, without loss of generality, be applied to other magnet designs. For example, in the magnet designed by the National Physical Laboratory in the United Kingdom [20], the vertical component of the magnetic flux in the gap can be reduced by decreasing the height of the inner yoke or adding an additional permanent magnet ring in the inner yoke.

ORCID iDs

Shisong Li https://orcid.org/0000-0002-2509-5523
Stephan Schlamminger https://orcid.org/0000-0002-9270-4018

References

[1] Kibble B P 1976 A measurement of the gyromagnetic ratio of the proton by the strong field method *Atomic Masses and Fundamental Constants* vol 5 (New York: Plenum) pp 545–51
[2] Haddad D *et al* 2016 A precise instrument to determine the Planck constant and the future kilogram *Rev. Sci. Instrum.* **87** 061301
[3] Mills I *et al* 2006 Redefinition of the kilogram, ampere, kelvin and mole: a proposed approach to implementing CIPM recommendation 1 (CI-2005) *Metrologia* **43** 227–46
[4] Li S *et al* 2012 Precisely measuring the Planck constant by electromechanical balances *Measurement* **45** 1–13
[5] Steiner R 2013 History and progress on accurate measurements of the Planck constant *Rep. Prog. Phys.* **76** 016101
[6] Stock M 2013 Watt balance experiments for the determination of the Planck constant and the redefinition of the kilogram *Metrologia* **50** R1–16
[7] Schlamminger S *et al* 2014 Determination of the Planck constant using a watt balance with a superconducting magnet system at the National Institute of Standards and Technology *Metrologia* **51** S15–24
[8] Li S *et al* 2016 Coil motion effects in watt balances: a theoretical check *Metrologia* **53** 817–28
[9] Li S *et al* 2016 A discussion of Bl conservation on a two dimensional magnetic field plane in watt balances *Meas. Sci. Technol.* **27** 051001
[10] Robinson I 2012 Towards the redefinition of the kilogram: a measurement of the Planck constant using the NPL Mark II watt balance *Metrologia* **49** 113–56
[11] Sanchez A *et al* 2014 A determination of Planck's constant using the NRC watt balance *Metrologia* **51** S5–14
[12] Stock M 2006 Watt balances and the future of the kilogram *INFOSIM Informative Bulletin of the Inter American Metrology System (November 2006)* pp 9–13
[13] Baumann H *et al* 2013 Design of the new METAS watt balance experiment Mark II *Metrologia* **50** 235–42
[14] Seifert F *et al* 2014 Construction, measurement, shimming, and performance of the NIST-4 magnet system *IEEE Trans. Instrum. Meas.* **63** 3027–38
[15] Gournay P *et al* 2005 Magnetic circuit design for the BNM watt balance experiment *IEEE Trans. Instrum. Meas.* **54** 742–5
[16] Kim D *et al* 2014 Design of the KRISS watt balance *Metrologia* **51** S96–100
[17] Sutton C *et al* 2014 A magnet system for the MSL watt balance *Metrologia* **51** S101–6
[18] Li S *et al* 2015 Field representation of a watt balance magnet by partial profile measurements *Metrologia* **52** 445–53
[19] Bielsa F *et al* 2015 Alignment of the magnetic circuit of the BIPM watt balance *Metrologia* **52** 775–82
[20] Robinson I A and Kibble B P 2007 An initial measurement of Planck's constant using the NPL Mark II watt balance *Metrologia* **44** 427–40